Article:

Clarke, SD and Hird, CC (2012) Modelling of viscous effects in natural clays. Canadian Geotechnical Journal, 49 (2). 129 - 140. ISSN 0008-3674

https://doi.org/10.1139/T11-084

Published paper

Clarke, SD and Hird, CC (2012) *Modelling of viscous effects in natural clays. Canadian Geotechnical* Journal, 49 (2). 129 - 140. ISSN 0008-3674
http://dx.doi.org/10.1139/T11-084

MODELLING OF VISCOUS EFFECTS IN NATURAL CLAYS

S. D. Clarke and C. C. Hird

The University of Sheffield

<u>*Contact address*</u>

Department of Civil and Structural Engineering

The University of Sheffield

Mappin Street

Sheffield

S1 3JD

Telephone: +44(0)114 2225703 Fax: +44(0)114 2225700

email: <u>sam.clarke@sheffield.ac.uk</u>

<u>Date revised:</u> September 2011

Word Count: 5192 excluding abstract

ABSTRACT

A new approach to allow the modelling of the viscous behaviour of natural clay soils, including creep, stress relaxation and the effects of applied strain rate on soil stiffness, has been developed based on the BRICK constitutive model (Simpson, 1992). The new model, SRD (Strain Rate Dependent) BRICK, was used in a series of simulations to demonstrate its capabilities in predicting realistic behaviour during one-dimensional compression and undrained triaxial tests in which applied strain rates were varied. Triaxial stress path tests conducted by Gasparre *et al*. (2007) to assess the influence of creep, resulting from recent stress history, on soil stiffness were also simulated. The observed trends concerning the stiffness at small strains were successfully modelled.

KEYWORDS

Constitutive Modelling, Stress History, Clay, Visco-plastic, BRICK, Strain

INTRODUCTION

Accurate predictions of ground displacements are essential for the success of complex construction projects in crowded urban environments, where existing structures must be safeguarded from the impact of new construction. Although sophisticated finite element analyses can be used to predict deformations, their accuracy depends on the quality of the underlying constitutive models. There is a continuing need to refine and improve these models.

The pre-failure deformation of overconsolidated clays, which underlie many cities, is known to be governed by their highly non-linear and mainly inelastic behaviour. Various constitutive models have been developed to allow the modelling of this behaviour (e.g. Al-Tabbaa & Wood, 1989; Jardine, 1992; Simpson, 1992; Whittle, 1993; Bolton *et al*. 1994; Stallebrass & Taylor, 1997; Grammatikopoulou *et al*. 2008) and laboratory testing is commonly performed to provide input parameters at small strain levels. Recent testing conducted on London Clay has shown that, not only is the small strain behaviour inelastic and non-linear, but it is also susceptible to the effects of creep and other viscous phenomena (Gasparre *et al*., 2007; Sorensen *et al*., 2007). Indeed, the need to take account of creep when conducting triaxial stress path tests is well recognised (e.g. Clayton and Heymann, 2001). It may be reasoned that such effects must also be modelled if truly accurate predictions of deformations are to be made, yet this is rarely done. Exceptionally, Kanapathipillai (1996) showed that by accounting for the effects of creep, the prediction of displacements around tunnels could be improved.

Strain rate dependent behaviour of clay soils, attributable to viscosity, is seen directly in constant rate of strain (CRS) one-dimensional compression tests, where different normal compression lines are obtained with different applied strain rates (e.g. Leroueil *et al*., 1985; 1996), and in undrained triaxial tests, where faster testing leads to increased strength (e.g. Vaid *et al*., 1979). In order to overcome the problem of natural variation between samples in a series of CRS tests, step change in strain rate (SRS) testing on a single sample can be used to investigate viscous effects at different strain rates. In tests on natural clays a change in strain rate leads to a persistent change in the stress level (e.g. Graham *et al*., 1983; Leroueil *et al*., 1985), termed isotach behaviour by Tatsuoka *et al*. (2002). This implies that there is a unique stress-strain curve, or isotache (Šuklje, 1957), for each strain rate. Other forms of viscous behaviour have been identified in tests on reconstituted clays and sands but, as these are not applicable to natural clays, they will not be considered here.

Until now, constitutive modelling of viscous behaviour has generally involved adapting time-invariant elasto-plastic models with yield surfaces formulated in stress space so that their response depends on the current rate of plastic strain. Examples of such approaches are given by Kutter and Sathialingam (1992), Yin *et al.* (2002), Rocchi *et al.* (2003), Hinchberger and Rowe (2005), and Kelln *et al.* (2009). However, use of the BRICK constitutive model (Simpson, 1992) permits a radically different approach. BRICK can be regarded as a multiple kinematic yield surface model but is developed within strain space and does not rely on classical plasticity concepts such as a plastic potential or a flow rule. This facilitates the creation of a model which is able to deal not only with the influence of complex stress history and the non-linear behaviour of geomaterials but also with the effects of strain rate. Of course, with this versatility comes the expense of determining a larger suite of parameters, some of which require advanced or time consuming testing.

This paper reports work done to incorporate the modelling of viscous effects, referred to above, into BRICK. The paper provides a brief description of the model, as originally developed, before proposing modifications to cater for viscosity. The performance of the modified model is then tested by simulating laboratory test results in the literature (Leroueil *et al*., 1985; Graham *et al*., 1983; Sorensen *et al*., 2007). Finally, tests conducted by Gasparre *et al*. (2007) are simulated with the aim of studying the influence of creep, resulting from recent stress history, on soil stiffness.

THE BRICK MODEL

The principles of the BRICK model are best explained using the analogue of a person walking around a room and dragging a series of bricks tied to them with separate strings of differing length. Each brick represents a proportion of the soil and each string length represents the amount of strain required to generate plasticity in that proportion of soil. The sides of the room are taken to be the axes of volumetric and shear strain. As the person moves through the strain space represented by the room (as strain is applied to the soil) initially all the strings are slack so the bricks remain stationary and the soil strains elastically; as the person moves further some bricks start to move too and there is some plastic strain. The more bricks that move, the higher is the proportion of soil undergoing plastic deformation and the lower the stiffness of the soil becomes. This trend is expressed by the stepped s-shaped curve used in BRICK to model the progressive reduction in stiffness with strain, Figure 1. In effect, each brick and its string define a yield surface in strain space for a portion of the soil. Stress changes are calculated from the elastic strains only but there is provision for stress levels to increase due to consolidation involving full plasticity. Stress history is accounted for by the current positions of the bricks relative to the person. To allow an accurate representation of stress history, the entire geological history of the soil is modelled back to when the soil was first deposited, including the deposition and erosion of the various overlying strata. The positions of the bricks give rise to a unique stiffness response which depends on the path followed when straining recommences. The failure surface in the BRICK model is loosely defined by the longest string length and the positions of the bricks relative to the current position of the person. All the strings must be taut in shear (i.e. all shear strain is plastic) for the model to predict “failure”.

Since it was first published, the BRICK model has been generalised to facilitate full 3D analyses by the inclusion of three extra components of shear strain (additional to the two shear components and one volumetric strain component required in the original BRICK model). The six components of strain and six conjugate stresses are listed in Appendix A1, and further details of the 3D model may be found in Ellison *et. al*. 2011.

MODELLING OF VISCOUS EFFECTS

Strain rate dependent string lengths

The modelling of viscous effects in the BRICK model can be achieved by making the string lengths strain rate dependent, as proposed by Sorensen (2006). In BRICK the string lengths are directly related to the soil strength, as a longer string length allows more elastic straining before the string becomes taut and the attached brick behaves plastically. This leads to a higher stiffness at any given stress level and hence a greater strength. If string length is taken to be proportional to soil strength, then equations developed previously to describe strain rate dependent strength can be applied to govern the string lengths in the modified model, named SRD (Strain Rate Dependent) BRICK. Many laws have been proposed to relate the undrained shear strength of a clay soil to the applied strain rate (e.g. Graham *et al*., 1983; Biscontin & Pestana, 2001; Di Benedetto *et al*., 2002; Einav & Randolph, 2006). Adapting one of these (Graham *et al*., 1983) and substituting string length for undrained shear strength, Sorensen (2006) proposed the following:

$$SL = SL_{ref}\left[1 + \beta\, ln\left(\frac{|\dot{\varepsilon}|}{\dot{\varepsilon}_{ref}} + 1\right)\right]$$

[1]

where SL = string length, SL_{ref} = reference string length, $\dot{\varepsilon}_{ref}$ = reference strain rate, $\dot{\varepsilon}$ = strain rate and β = rate sensitivity coefficient (Tatsuoka 2005).

Importantly, this equation only affects moving bricks, i.e. those proportions of the soil undergoing plastic strain, and hence $\dot{\varepsilon}$ is a plastic strain rate calculated from the movement of the bricks on a brick by brick basis. The brick strain rate is also deemed to be the vectorial strain rate of the individual brick as calculated in Equation 2:

$$\dot{\varepsilon} = \sqrt{(\dot{v})^2 + (\dot{\gamma})^2}$$

[2]

where $\dot{v}$ = volumetric strain rate, $\dot{\gamma}$ = vectorial shear strain rate. It should be noted that for three-dimensional applications the vectorial shear strain rate is calculated as the root sum of the five shear components of strain shown in Appendix A1.

Before Equation 1 can be used, a reference set of string lengths must be specified, along with a reference strain rate. String lengths may be obtained by measuring the degradation of stiffness after a 180° change in the direction of the stress path in a laboratory test. Such tests are generally conducted at a much higher strain rate than the reference strain rate. However, as long as the strain rate, $\dot{\varepsilon}_{test}$, at which the test takes place is known, the reference string lengths can be back calculated using Equation 3, with the testing string lengths, SL_{test}, being defined by a stepwise approximation to the generated stiffness degradation curve (Figure 1). Elastic strains may usually be neglected in specifying $\dot{\varepsilon}_{test}$.

$$SL_{ref} = \frac{SL_{test}}{1 + \beta \ln(\dot{\varepsilon}_{test}/\dot{\varepsilon}_{ref} + 1)}$$

[3]

Equation 1 governs the change in string lengths for strain rates that are normally above the reference strain rate. For rates below the reference strain rate, the string lengths converge on the reference string lengths as the strain rate drops to zero.

Control of strain rate changes

Alone, Equation 1 is able to model persistent effects of strain rate increases and decreases but without some other control all the effects would be instantaneous. This would preclude the modelling of creep and stress relaxation.

The control of the maximum rate of strain rate reduction is based on an equation presented by Singh & Mitchell (1968) describing the natural decay of strain rate with time under constant stress conditions, a simplification of which is

$$\dot{\varepsilon} = A\left(\frac{t_1}{t}\right)^m$$

[4]

where A = strain rate at some arbitrarily chosen time, t_1, m = negative of the slope of the relationship between the logarithm of strain rate and the logarithm of time, and t = current time. In SRD BRICK whenever the applied strain rate is decreased, it is assumed that the reduction in the rate of plastic strain cannot exceed that predicted by a relationship of this form. If the applied strain reduces at a faster rate, there is some degree of stress relaxation arising from plastic movement of bricks relative to the person, caused by the shortening of strings, and a compensating release of elastic strain. Of course, pure stress relaxation can be predicted by holding the soil at constant strain, which corresponds to a stationary person in the analogue. To achieve pure creep behaviour (increasing strain at constant stress) the movement of the bricks induced by the shortening of the string lengths must be balanced by the movement of the person so that no stress change is predicted.

To calculate the decay of strain rate from a logarithmic relationship, such as Equation 4, the time since the start of the decay must be known. Here there is a difficulty in that the BRICK model is implemented in an incremental routine (coded by Simpson (1992)) that does not track the passage of time and hence both t and t_1 in Equation 4 are unknown. However, at any stage the string lengths during the previous time increment, SL_{prev}, are known and so the previous strain rate, $\dot{\varepsilon}_{prev}$, can be calculated by rearranging

Equation 1 and substituting $\dot{\varepsilon}_{\text{prev}}$ for $\dot{\varepsilon}$:

$$\dot{\varepsilon}_{prev} = \dot{\varepsilon}_{ref}\left(e^{\left(\frac{\left(\frac{SL_{prev}}{SL_{ref}}\right)-1}{\beta}\right)} - 1\right)$$

[5]

If the period over which the strain rate is decreasing at its maximum rate is set to have an upper limit and a specific strain rate (i.e. the reference strain rate) is associated with that limit, each strain rate can be associated with a unique time as shown in Figure 2. Presently it will be assumed that the upper time limit, t_{max}, is 10^8 seconds which roughly equates to 31 years and 8 months and may be considered sufficiently long to model creep or stress relaxation in most practical applications. Based on test data for London Clay from Bishop (1966), the strain rate at this time would be $1\text{x}10^{-13}\text{s}^{-1}$. Later this will be adopted as the reference strain rate. Also, by fitting Equation 4 to the same data a value of m =1.039 can be found.

Knowing $\dot{\varepsilon}_{\text{prev}}$ the corresponding time governing the subsequent decay of strain rate can be calculated as follows:

$$t_{prev} = 10^{\left(\log(t_{max}) - \left(\log\left(\frac{\dot{\varepsilon}prev}{\dot{\varepsilon}_{ref}}\right)m\right)\right)}$$

[6]

where t_{prev} = time at the end of the previous BRICK increment. The current strain rate predicted by the logarithmic decay can then be calculated by introducing an incremental measure of time into BRICK, δt, so that the current time $t = t_{prev} + \delta t$ and

$$\dot{\varepsilon} = 10^{\log(\dot{\varepsilon}_{ref}) + \max\left(0\,,\left(\frac{\log(t_{max}) - \log(t)}{m}\right)\right)}$$

[7]

With the reduced strain rate for each brick thus determined, the corresponding string length can be calculated using Equation 1.

While it is clearly necessary to control the rate of strain rate reduction (string shortening), it would not be unrealistic to assume that the effect of an increase in strain rate (string lengthening), manifested as an increase in stiffness, is instantaneous. However, it has been found that implementing such an assumption leads to numerical instabilities. Therefore, responses to strain accelerations are governed by Equation 8 which smoothes the convergence of the current string lengths upon the longer target string lengths:

$$\delta SL = \alpha\left(SL_{target} - SL_{prev}\right)$$

[8]

where α = convergence factor (0.5), SL_{target} = the string lengths calculated during the current BRICK increment. As the response takes place over a series of increments, the incremental time, as well as α, affects the behaviour. For the simulations in this paper the incremental time was 1 second and responses were substantially complete in a few seconds.

Appendix A2 contains a guide to the implementation of the SRD BRICK model in a computer program.

MODEL PARAMETERS

The BRICK model requires appropriate stiffness parameters to define the behaviour of a given soil. As shown previously, the shape of the stiffness degradation curve is defined in a stepwise manner by a series of vectorial strains (string lengths) and soil proportions. Ideally, the stiffness degradation would be fitted to experimental data but, where suitable data are not available, modelling can be based on a set of string lengths for London Clay proposed by Simpson (1992). For simplicity these can be scaled by a constant factor to suit a given soil, thereby translating the curve shown in Figure 1 while preserving its shape (the step heights remain unchanged). Typically, ten steps are considered sufficient to capture the shape of the degradation curve.

The BRICK model also requires Cam Clay style parameters, λ^* and κ^*, to define the compression and swelling lines, these parameters being defined in terms of volumetric strain rather than voids ratio. A further parameter, ι, is also required to govern the very small strain (elastic) stiffness. For the SRD modification to the BRICK model, three extra parameters are required: the reference strain rate ($\dot{\varepsilon}_{ref}$), the decay constant (m) and the rate sensitivity coefficient (β). For the simulations reported in this paper, a reference strain rate of $1\text{x}10^{-13}\ s^{-1}$ has been used, along with a decay constant of 1.039. In most cases the rate sensitivity coefficient could then be fitted to the observed strain rate behaviour.

SIMULATED BEHAVIOUR PATTERNS

In order to explore the capabilities of the SRD BRICK model, a number of published experiments were simulated.

Simulation of one-dimensional step rate of strain compression tests

The SRD BRICK model was first used to simulate SRS tests under one-dimensional compression, as conducted on natural Batiscan Clay by Leroueil *et al.* (1985). The physical tests demonstrated isotach behaviour, so that a change in applied strain rate led to a persistent change in the stress level for a given volumetric strain. The simulations incorporated the modelling of the stress history of the soil with a preconsolidation pressure of 88 kPa and an estimated in-situ vertical effective stress of 65 kPa. The model parameters are shown in Table 1. The λ^* value was fitted to the gradient of the compression lines in Leroueil *et al*. (1985) when re-plotted on a logarithmic scale of effective vertical stress, Figure 3. The test procedure followed in the simulation is given in Table 2. For structured soils, such as natural Batiscan Clay, the approximation of a linear relationship is only valid over a limited strain range. Thus, in Figure 3 the physical and simulation data are seen to agree well up to 13% volumetric strain but then to diverge. The transitions between isotache lines are well predicted, with both the controlled increase in strain rate (Equation 7) and decrease in strain rate (Equation 6) showing realistic behaviour when compared with the physical test data.

Simulation of triaxial step rate of strain and relaxation tests

Graham *et al*. (1983) reported results of an undrained SRS triaxial test on a sample of natural Belfast Clay. During two relaxation periods the stresses on the sample were allowed to relax while the axial strain was maintained. The duration of each test stage was back calculated from Figure 4(a). Table 3 gives details of the test stages and Table 1 again lists the model parameters used. The stress history of the Belfast Clay was modelled by consolidating the soil to an effective vertical stress of 60 kPa and then allowing it to swell back to an estimated in-situ vertical effective stress of 40 kPa. This gave an overconsolidation ratio of 1.5 which lies within the range of 1.2-1.8 quoted by Crooks & Graham (1976). The λ* and κ* values were back calculated from the data given in Crooks & Graham (1976).

Figure 4 shows a comparison between the stress strain curve presented in Graham *et al*. (1983) and that generated by the SRD BRICK model (σ'_{vo} = in situ vertical effective pressure). It can be seen that generally the comparison is very good with similar behaviour being observed during both the step changes in strain rate and the relaxation periods. This demonstrates that the SRD model is able to predict strain rate dependent behaviour in undrained shearing. The strain softening of the soil at axial strains of more than 2% is not predicted well, although this is a deficiency of the underlying BRICK model rather than the SRD adaptation.

Sorensen et al. (2007) conducted undrained SRS triaxial tests on natural London Clay samples which were found to exhibit isotach behaviour. The samples were taken from between 13.95 m and 15.45 m below ground level at the Heathrow Terminal 5 site. From Gasparre (2005) the unit weight of the London Clay (for the same horizon) is 19.4 kN/m^3. This leads to an estimated insitu mean effective stress of between 283 and 303 kPa, assuming a K_0 value of 1.88 (Gasparre, 2005) and the water table to lie at a depth of 4.5m. At the sampling depth Sorensen (2006) estimated that the previous overburden pressure was around 2 MPa based on results presented in Skempton & Henkel (1957). This gives a previous maximum mean effective stress of approximately 1440 kPa, based on a K_0 value of 0.58 (Simpson, 1992). The above information was used to model the stress history of the soil prior to testing. In addition to step changes of axial strain rate ($\dot{\varepsilon}_a$), the tests involved some small unload/reload cycles, the details of which are given in Table 4. As before, the model parameters for this simulation are given in Table 1 where the reference string lengths are taken to be half the Simpson (1992) lengths. This latter assumption was necessitated by a lack of information to allow the determination of the in-situ reference stiffness degradation curve and was based on some previous experience of modelling creep effects in London Clay (Kanipathipillai, 1996). However, further work suggests that results for behaviour at practically relevant strain rates may be relatively insensitive to this assumption (Clarke, 2009).

Figure 5(a) shows the pre-peak behaviour of a natural sample during the SRS test and Figure 5(b) shows the prediction of the SRD BRICK model. It can be seen, once again, that the two compare well. The effects of the step changes in strain rate are accurately simulated, although the regain of stress after unloading takes longer in the simulation. It should be noted that the period of creep immediately prior to some of the unload–reload cycles was left out of the simulation as the focus was to determine the rate sensitivity co-efficient β for London Clay (0.23) for use in the simulation of the Gasparre *et al*. (2007) test series. By comparison of Figures 4 and 5 it can be seen, as would be expected, that in the more heavily overconsolidated soil the rate effects are less pronounced.

THE INFLUENCE OF RECENT STRESS HISTORY AND CREEP ON STIFFNESS

It was shown by Atkinson *et al*. (1990) that the initial stiffness of overconsolidated clay soil observed, for example, in a triaxial test depends on the direction of the stress path followed to reach the initial stress state in the test. A larger change of direction from the approaching to the testing stress path results in a higher initial stiffness. This behaviour was reproduced by the original BRICK model (Simpson 1992). However, in later tests conducted by Clayton & Heymann (2001) the stiffness response was found to be independent of the degree of rotation in the stress path. Critically the tests conducted by Atkinson *et al*. (1990) and Clayton & Heymann (2001) utilised different methodologies. Atkinson *et al*. (1990) used long approach stress paths (90 kPa on a conventional plot of deviator stress, q, versus mean effective normal stress, p') and allowed 3-4 hours rest between test stages (Richardson, 1988), whereas Clayton and Heymann (2001) used shorter approach paths and a period of 6-12 days to allow for the decay of creep.

The effects of creep and the length of the approach stress path were investigated by Gasparre *et al*. (2007) to better understand the relationship between creep and the effects of recent stress history. In triaxial tests on natural London Clay samples it was found that a period of creep can eliminate the effects of the recent stress history (as found by Clayton & Heymann (2001)), providing the approach path length is less than 10 kPa, Figure 6(a) in which G is the tangential stiffness and ε_s is the shear strain, $2(\varepsilon_a - \varepsilon_r)/3$ (ε_a= axial strain and ε_r= radial strain). If creep is not allowed after similarly short approach paths, then the results show the same trend as seen by Atkinson *et al*. (1990), Figure 6(b). Gasparre *et al*. (2007) also showed that for longer (100kPa) approach paths the influence of the recent stress history was soon evident even when creep was allowed to occur, Figure 6(c).

The tests performed by Gasparre *et al*. (2007) were simulated using the SRD BRICK model. The stages followed in the simulation are given in Table 5 and included modelling the geological stress history of the soil, the sampling process (albeit in a simplified manner) and the triaxial testing which itself was split into separate stress and strain controlled stages. In test stages involving creep, stresses were held constant for a number of days as creep strains decayed. In stages without creep, stresses were only held constant for three hours, in line with the procedure used by Atkinson *et al*. (1990). The geological stress history was modelled in the same manner as in the simulation of the test by Sorensen (2006), described above. During this stage viscous effects were not explicitly modelled but the string lengths were set equal to their shortest (reference) values. Had viscous effects been explicitly modelled, due to the large times involved, the effects of creep would soon have led to the string lengths reducing to these reference values.

As the Gasparre *et al*. (2007) tests were conducted on natural samples of London Clay, suitable parameters for the SRD BRICK model, Table 6, were determined by referring to previous experience and available laboratory data. The values of β, m and reference strain rate were taken from the simulation of the work done by Sorensen *et al.* (2007), while the string lengths were fitted to stiffness degradation data obtained by Gasparre (2005), Figure 7. The fit deviates in the very small strain region to take account of the elastic shear modulus, G_{max}, measured using bender elements. Figure 7 also shows a comparison between the BRICK parameters given in Simpson (1992) and those fitted to Gasparre's data. The former can be seen to allow higher strains before the stiffness starts to degrade, possibly because they were derived from back analysis of geotechnical structures rather than laboratory testing. Given that Gasparre's results were obtained on similar samples to those in the tests being simulated, they were considered the most appropriate ones to use. Equation 2 was used to calculate the reference string lengths, with the fitted stiffness degradation curve from Figure 7 providing the testing string lengths (SL_{test}). The axial strain rate used to generate the stiffness degradation curve was assumed to be 0.0025%/h, similar to the rate achieved in the tests being simulated. While the λ* and κ* values were taken directly from Simpson (1992), the value of ι was chosen so as to predict the maximum stiffness shown in Figure 7. It may be noted that once the model parameters shown in Table 6 had been determined, before starting the simulations, no adjustments were subsequently made.

Short approach path with the effects of creep

This simulation aimed to produce results for comparison with those shown in Figure 6(a). Following the earlier stages (1-5a in Table 5), approach paths were followed in both compression and extension directions before creep was allowed during a long holding period. The stiffness was then evaluated during the extension undrained shearing stage and the tangential stiffness was plotted against shear strain, Figure 8(a). Qualitative agreement between Figures 8(a) and 6(a) is reasonably good.

Figure 8(a) shows that the SRD BRICK model can successfully simulate the erasing of recent stress history effects by creep, given the close match of the curves for low and high stress path rotations. This behaviour can be understood in terms of the analogue for the BRICK model. After a period of movement by the person, in the unmodified BRICK model some of the strings attached to bricks that are currently moving are likely to remain taut if the person continues to move (unless there is a complete reversal of their direction) giving rise to some plastic strain. In SRD BRICK, during the simulated creep period, all the taut strings shorten with time (thus moving at least some bricks) but, when the person's movement accelerates, any taut strings lengthen again. Initially, therefore, the response of the soil is wholly elastic and is generally stiffer than it would have been had it not been for the holding period. As the bricks do not move a large amount during the short approach paths, creep is able to erase the effects easily.

Short approach path without the effects of creep

This simulation was identical to the previous one except that, after completion of the approach stress paths, only a short holding period was allowed severely restricting the occurrence of creep. The results shown in Figure 8(b) may be compared with the experimental data in Figure 6(b). In both cases a higher stress path rotation produces a higher initial stiffness showing the influence of recent stress history, as described by Atkinson *et al*. (1990). However, after a shear strain of about 0.01% the difference effectively disappears as the influence of the common, earlier stress history asserts itself. Again, qualitative agreement between simulation and experiment is reasonably good, although the experimental data display scatter at very small strains and there is an unexpected peak in the high rotation curve at about 0.003% strain. In terms of the analogue, in the low rotation test some strings are still taut, whereas in the high rotation test, with the direction of movement reversed, the same strings are initially slack leading to a higher stiffness.

Long approach path with the effects of creep

The final simulation was identical to the first one except that the approach stress paths were much longer. The simulated and experimental results are shown in Figures 8(c) and 6(c) respectively. Although agreement is perhaps less good than in the other two cases, the trends are still matched. Due to creep, the initial stiffness is almost the same for both low and high stress path rotations, but as strains increase the expected influence of previous stress history reasserts itself and the curves diverge. This shows that creep cannot completely erase, for example, the effect of the soil's geological stress history. As in the first case, the creep period acts to shorten the string lengths allowing elastic straining in all directions following the approach paths. As many bricks were moved a large amount during these approach paths, creep cannot fully erase the effects and hence the stiffnesses diverge as the bricks on longer strings become engaged once more.

CONCLUSIONS

In this paper a new approach to the modelling of viscous behaviour of natural clays has been presented, based on the BRICK model (Simpson, 1992). As originally proposed by Sorensen (2006), viscous effects are modelled by allowing the current strain rate to dynamically affect the length of the strings in BRICK. The modified model has been called SRD (Strain Rate Dependent) BRICK. Controls are placed on the maximum rate of string length reduction using a function derived from the work of Singh & Mitchell (1968) in order to model effects such as creep and stress relaxation. Increases of string length are achieved almost instantaneously.

The SRD BRICK model was able to simulate convincingly the isotach strain rate behaviour (Tatsuoka *et al*. 2002) observed as strain rates were varied during one-dimensional compression tests by Leroueil *et al*. (1985) and during undrained triaxial tests by Graham *et al*. (1983) and Sorensen *et al*. (2007).

A series of tests by Gasparre *et al*. (2007), aimed at investigating the effects of creep and recent stress history on soil stiffness, was also simulated. Trends in the experimental observations were well reproduced and it was confirmed that creep can erase the effect of recent stress history, but only if the recent stress paths are sufficiently short.

Experience is now required of applying the SRD BRICK model to case histories of construction in the course of which it should be possible to determine the significance of viscous effects. Following the work described here, the SRD BRICK model has been implemented in a finite element program and used to back analyse two construction projects in London where the fit of the analysis was improved by incorporating viscous effects (Clarke, 2009). A further paper describing this experience is in preparation.

ACKNOWLEDGEMENTS

The Authors would like to thank Dr Brian Simpson of Arup Geotechnics for his interest in the work and many helpful discussions. The first Author was supported with an EPSRC Doctoral Training Award.

NOTATION

A = strain rate at some arbitrarily chosen time, t_1,
G = tangential shear modulus
G_{max} = elastic shear modulus
K_0 = lateral earth pressure coefficient at rest
m = negative of the slope of the relationship between the logarithm of strain rate and the logarithm of time
p' = mean effective normal stress, $(\sigma'_a + 2\sigma'_r)/3$
q = deviator stress, $(\sigma_a - \sigma_r)$
SL = string length
SL_{prev} = previous string length
SL_{ref} = reference string length
SL_{target} = the string lengths calculated during the current BRICK increment
SL_{test} = testing string length
t = current time
t_{max} = upper limit to the time allowed for creep

t_{prev} = time in seconds at the end of the previous BRICK increment.
δt = time increment
v = volumetric strain
$\dot{v}$ = volumetric strain rate

α = decay factor
β = rate sensitivity coefficient
$\dot{\gamma}$ = vectorial shear strain rate
ι = parameter governing elastic modulus
κ^* = gradient of the swelling and recompression line
λ^* = gradient of the normal compression line
$\dot{\varepsilon}$ = applied strain rate
$\dot{\varepsilon}_{test}$ = testing strain rate
ε_a = axial strain
$\dot{\varepsilon}_a$ = axial strain rate
ε_r = radial strain
$\dot{\varepsilon}_{ref}$ = reference strain rate
ε_s = shear strain, $2(\varepsilon_a - \varepsilon_r)/3$
$\dot{\varepsilon}_{test}$ = testing strain rate
σ_1 = major principal stress
σ_3 = minor principal stress
σ'_v = vertical effective stress
σ'_{vo} = in situ vertical effective stress

REFERENCES

Al-Tabbaa, A. and Wood, D. M. 1989. An experimentally based 'bubble' model for clay, *NUMOG 3, Niagra Falls* pp. 91‑99.

Atkinson, J. H., Richardson, D. and Stallebrass, S. E. 1990. Effect of recent stress history on the stiffness of overconsolidated soil, *Géotechnique* **40**, No. 4: 531–540.

Bolton, M. D., Dasari, G. R. and Britto, A. M. 1994. Putting small strain non-linearity into Modified Cam Clay model.

Biscontin, G. and Pestana, J. M. 2001. Influence of peripheral velocity on vane shear strength of an artificial clay, *Geotechnical Testing Journal* **24**, No. 4: 423–429.

Clarke, S. D. 2009. Enhancement of the BRICK constitutive model to incorporate viscous effects, PhD Thesis, University of Sheffield.

Clayton, C. R. I. and Heymann, G. 2001. Stiffness of Geomaterials at very small strains, *Géotechnique* **51**, No. 3: 245–255.

Crooks, J. H. A. and Graham, J. 1976. Geotechnical properties of the Belfast estuarine deposits, *Géotechnique* **26**, No. 2: 293–315.

Di Benedetto, H., Tatsuoka, F. and Ishihara, M. 2002. Time-dependent shear deformation characteristics of sand and their constitutive modelling, *Soils and Foundations* **42**, No. 2: 1–22.

Einav, I. and Randolph, M. 2006. Effect of strain rate on mobilised strength and thickness of curved shear bands, *Géotechnique* **56**, No. 7: 501–504.

Ellison, K., C., Soga, K. and Simpson, B. 2011. A strain space soil model with evolving stiffness anisotropy. Submitted to Geotechnique.

Gasparre, A. 2005. *Advanced laboratory characterisation of London Clay*, PhD Thesis, Imperial College London.

Gasparre, A., Nishimura, S., Minh, N. A., Coop, M. R. and Jardine, R. J. 2007. The stiffness of natural London Clay, *Géotechnique* **57**, No. 1: 33–47.

Graham, J., Crooks, J. H. A. and Bell, A. L. 1983. Time effects on the stress-strain behaviour of natural clays, *Géotechnique* **33**, No. 3: 327–340.

Grammatikopoulou, A., Zdravkovic, L. and Potts, D. M. 2008. The influence of previous stress history and stress path direction on the surface settlement trough induced by tunnelling, *Géotechnique* **58**, No. 4: 269-281.

Hinchberger, S. D. and Rowe, R. K. 2005. Evaluation of the predictive ability of two elastic-viscoplastic constitutive models, *Canadian Geotechnical Journal* **42**: 1675–1694.

Jardine, R. J. 1992. Some observations on the kinematic nature of soil stiffness, *Soils and Foundations* **29**, No. 3: 436–447.

Kanapathipillai, A. 1996. *Review of the Brick model of soil behaviour*, MSc Thesis, Imperial College, London.

Kelln, C., Sharma, J., Hughes, D. and Graham, J. 2009. Finite element analysis of an embankment on a soft estuarine deposit using an elastic-viscoplastic soil model, *Canadian Geotechnical Journal* **46**: 357–368.

Kutter, B. L. and Sathialingam, N. 1992. Elastic-viscoplastic modelling of the rate-dependent behaviour of clays, *Géotechnique* **42**, No.3: 427-441

Leroueil, S., Kabbaj, M., Tavernas, F. and Bouchard, R. 1985. Stress-strain-strain rate relation for the compressibility of sensitive natural clays, *Géotechnique* **35**, No. 2: 159–180.

Richardson, D. 1988. *Investigations of threshold effects in soil deformations*, PhD Thesis, City University, London.

Rocchi, G., Fontana, M. and Da Prat, M. 2003. Modelling of natural soft clay destruction processes using viscoplasticity theory, *Géotechnique* **53**, No. 8, 729–745.

Simpson, B. 1992. Retaining structures: displacement and design, *Géotechnique* **42**, No. 4: 541–576.

Singh, A. and Mitchell, J. K. 1968. General stress-strain-time function for soils, *Journal of the Soil Mechanics and Foundations Division, ASCE* **94**, No. SM1: 200–220.

Skempton A. W. and Henkel D. J. 1957. Tests on London Clay from deep borings at Paddington, Victoria and the South Bank. *Proc. 4th Int. Conf. S.M. and F.E., London, 1, pp. 100-106.*

Sorensen, K. 2006. *Influence of viscosity and ageing on the behaviour of clays,* PhD Thesis, University College London.

Sorensen, K. K., Baudet, B. A. and Simpson, B. 2007. Influence of structure on the time-dependent behaviour of a stiff sedimentary clay, *Géotechnique* **57**, No. 1: 113–124.

Stallebrass, S. E. 1990. The effect of recent stress history on the deformation of overconsolidated soils. PhD Thesis, City University, UK.

Stallebrass, S. E. and Taylor, R. N. 1997. The development and evaluation of a constitutive model for the prediction of ground movements in overconsolidated clay, *Géotechnique* **47**, No. 2: 235–253.

Tatsuoka, F. 2005. Effects of viscous properties and ageing on the stress-strain behaviour of geomaterials. *ASCE Geotechnical Special Publication* **143**, 1-60.

Tatsuoka, F. 2007. Keynote lecture: Inelastic deformation characteristics of geomaterial, *Soil stress-strain behaviour: measurement, modelling and analysis. Proceedings of the Geotechnical Symposium, Rome, 2006* pp. 1–108.

Tatsuoka, F., Ishihara, M., Di Benedetto, H. and Kuwano, R. 2002. Time-dependent shear deformation characteristics of geomaterials and their simulation, *Soils and Foundations* **42**, No. 2: 531–540.

Vaid, Y. P., Robertson, P. K. and Campanella, R. G. 1979. Strain rate behaviour of Saint-Jean-Vianney clay, *Canadian Geotechnical Journal* **16**: 34–42.

Whittle, A. J. 1993. Evaluation of a constitutive model for overconsolidated clays, *Géotechnique* **43**, No. 2: 289–313.

Yin, J.-H., Zhu, J.-G. and Graham, J. 2002. A new elastic viscoplastic model for time-dependent behaviour of normally and overconsolidated clays: theory and verification, *Canadian Geotechnical Journal* **39**: 157–173.

APPENDIX A1

Generalised strain components and associated stresses

For 3D applications the 6 components of strain are:

Volumetric strain		$v = \varepsilon_x + \varepsilon_y + \varepsilon_z$
Shear strain component	1	$g_{zx} = \varepsilon_z - \varepsilon_x$
Shear strain component	2	$g_y = (2\varepsilon_y - \varepsilon_x - \varepsilon_z)/\sqrt{3}$
Shear strain component	3	γ_{xy}
Shear strain component	4	γ_{yz}
Shear strain component	5	γ_{zx}

where x, y and z are Cartesian coordinate axes.

The following components of stress are respectively linked through the appropriate elastic moduli:

Mean stress		$p = (\sigma_x + \sigma_y + \sigma_z)/3$
Shear stress component	1	$t_{zx} = (\sigma_z - \sigma_x)/2$
Shear stress component	2	$t_y = (2\sigma_y - \sigma_x - \sigma_z)/2\sqrt{3}$
Shear stress component	3	τ_{xy}
Shear stress component	4	τ_{yz}
Shear stress component	5	τ_{zx}

APPENDIX A2

Implementation guide for the SRD BRICK model (to be read in conjunction with Simpson (1992) and Ellison et al. (2011))

The BRICK model is implemented as an iterative routine which identifies the stress changes produced by a given strain increment. Implementing a second iterative routine within the first one, to deal with the plastic strain rate dependency of the string lengths, could prove computationally expensive. This can be avoided by determining the modified string lengths (Equation 1) in only the first iteration of the BRICK routine.

Pass the applied strain increment into the BRICK routine, then:

1.) For each brick individually:
    a. Calculate all 6 components of the current plastic strain (Appendix A1) based on the applied strain, current brick position and reference string lengths.
    (Note the reference lengths are normally substantially shorter than those in the final iteration.)
    b. Calculate $\dot{\varepsilon}$ using Equation 2
    c. During the first BRICK iteration calculate the modified SRD string length, *SL* using the SRD subroutine:

    d. Enter SRD subroutine:
        i. Set convergence criteria for the SRD subroutine as 10% of the reference string length, SL_{ref}. This is a check on the variation in the calculated *SL* per SRD subroutine iteration.
        ii. Redefine $\dot{\varepsilon}$ using Equation 2.
        iii. Record the current string length, SL_{prev}.
        iv. Calculate *SL* using Equation 1.
        v. If $SL > SL_{prev}$, calculate $SL=SL_{prev} + (SL-SL_{prev})*\alpha$
        where α is the convergence factor (Equation 8).
        vi. If $SL < SL_{prev}$ apply Equation 5 to predict the previous strain rate, $\dot{\varepsilon}_{\text{prev}}$.
        Using $\dot{\varepsilon}_{\text{prev}}$ calculate t_{prev} using Equation 6.
        Calculate the current time, $t = t_{prev} + \delta t$.
        Calculate the decayed $\dot{\varepsilon}$ using Equation 7.
        vii. Modify the position of the brick to account for changing *SL*
        viii. Define error as $|SL - SL_{prev}|$
        ix. Repeat (i-ix) until convergence, as defined in (i)
    e. Exit SRD subroutine

2.) With the modified string lengths derive the associated elastic strains and hence stress changes.
3.) Repeat (1-3) until stress convergence is reached.

MATLAB code for the SRD BRICK model is given in Clarke (2009).

List of Tables

List of Figures / Captions

BRICK parameter		Leroueil *et al.* (1985)	Graham *et al.* (1983)	Sorensen *et al.* (2007)
Reference string length factor	SL_{ref} / SL_{LC}	0.050	0.50	0.50
Lambda*	λ^*	0.60	0.37	0.10
Kappa*	κ^*	0.030	0.054	0.020
Iota	ι	0.0041	0.0041	0.0029
Time decay constant	m	1.039		
Maximum creep time	t_{max}	10^8 s		
Reference strain rate	$\dot{\varepsilon}_{ref}$	$1\text{x}10^{-13}$ s^{-1}		
Rate sensitivity coefficient	β	0.1	1	0.23
The string lengths are initially slack and the original position of all the bricks lies at the origin. SL_{LC} are the original London Clay string lengths given in Simpson (1992). The step heights remain unchanged unless stated and are also given in Simpson (1992).				

Volumetric strain rate (%/h)	Strain limit (% volumetric strain)
0.97	3.7
0.038	7.2
0.97	12.1
0.038	23.5
0.97	25.7

Axial strain rate (%/h)	Strain limit (% axial strain)
0.5	6.0
Relaxation	-
0.5	7.8
5.0	10.0
0.5	12.5
0.05	13.5
5.0	15.8
0.5	18.0
0.05	18.5
0.5	19.0
Relaxation	-
0.5	20.0

Shear strain rate (%/h)	Strain limit (% shear strain)
0.05	0.58
Unload - reload	
0.80	0.68
0.05	0.80
0.80	0.92
0.20	1.02
0.05	1.11
0.80	1.34
Unload - reload	
0.80	1.63
0.05	2.31
Unload - reload	
0.80	2.73
0.20	2.91
0.05	3.00

Natural	Strain control	Stage 1	1D compression up to the geological maximum mean effective stress of 1442 kPa.
		Stage 2	1D swelling to the in-situ mean effective stress of 330kPa.
Sampling	Stress control	Stage 3	Stress path directly taking the soil from the insitu mean stress (330kPa) to the pre-test mean stress of 171kPa (17SH) or 136kPa (17.3SH) with a deviator stress of zero. Creep strains are generated during this stage.
Triaxial	Stress control	Stage 4	Isotropic consolidation back to the in-situ mean stress of 330kPa with a small deviator stress being applied dependent on the test to be conducted. Creep allowed.
		Stage 5a	Outgoing approach paths conducted under constant mean stress. This affects the magnitude and direction of the approach path for the final stage stiffness. Creep allowed.
		Stage 5b	Incoming approach path. Creep allowed.
	Strain control	Stage 6a	Dissipation of creep strains generated during the approach paths, if allowed (12 hours).
		Stage 6	Undrained extension or compression test.

BRICK parameter	Identifier	Value
Reference string lengths	SL_{ref}	5x10^{-7}, 1.5x10^{-6}, 3.125x10^{-6}, 5x10^{-6}, 1x10^{-5}, 1.75x10^{-5}, 2.5x10^{-5}, 3.5x10^{-5}, 5x10^{-5}, 0.0001, 0.0002, 0.00035, 0.0005, 0.001, 0.002, 0.004, 0.01, 0.0323
Stiffness reduction	G / G_{max}	0.9, 0.85, 0.815, 0.79, 0.74, 0.69, 0.61, 0.5, 0.4, 0.3, 0.22, 0.17, 0.13, 0.09, 0.06, 0.02, 0.009, 0
Lambda*	λ*	0.1
Kappa*	κ*	0.02
Iota	ι	0.0054
Time decay constant	m	1.0386
Reference strain rate	$\dot{\varepsilon}_{ref}$	1e^{-13}s^{-1}
Maximum creep time	t_{max}	10^{8} s
Rate sensitivity coefficient	β	0.23
The string lengths are initially slack and the original position of all the bricks lies at the origin.		

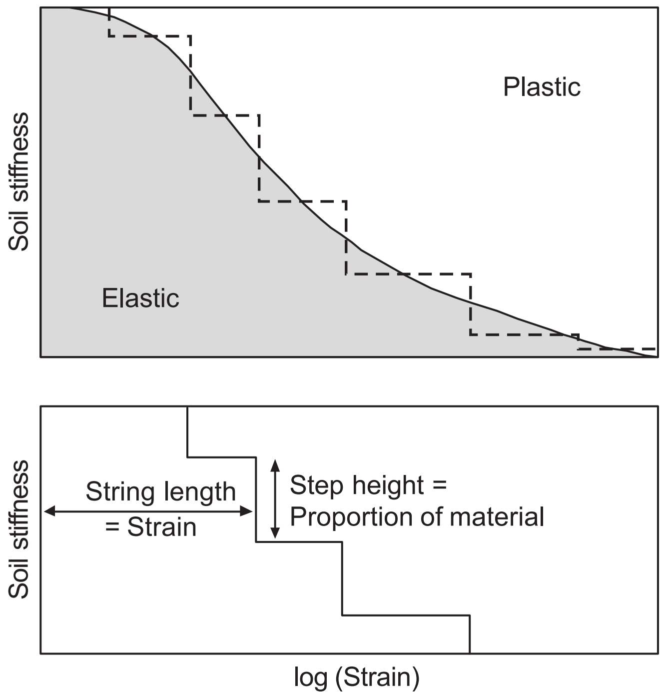
Plastic
Elastic
Soil stiffness
String length
= Strain
Step height =
Proportion of material
Soil stiffness
log (Strain)

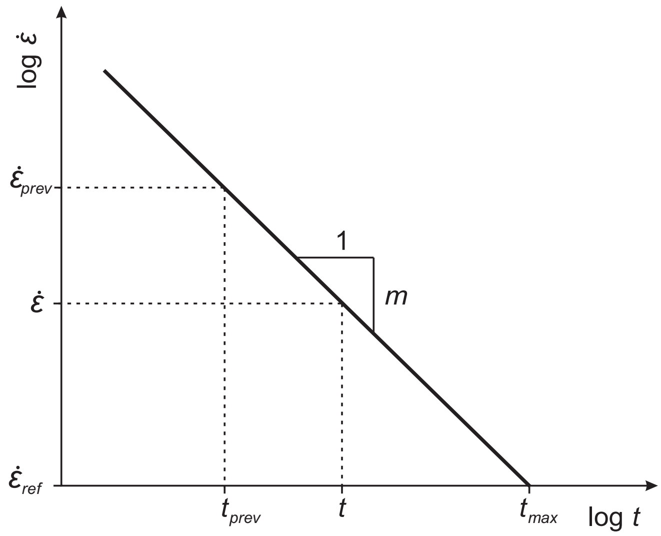
log $\dot{\varepsilon}$
$\dot{\varepsilon}_{prev}$
$\dot{\varepsilon}$
$\dot{\varepsilon}_{ref}$
1
m
t_{prev}
t
t_{max}
log t

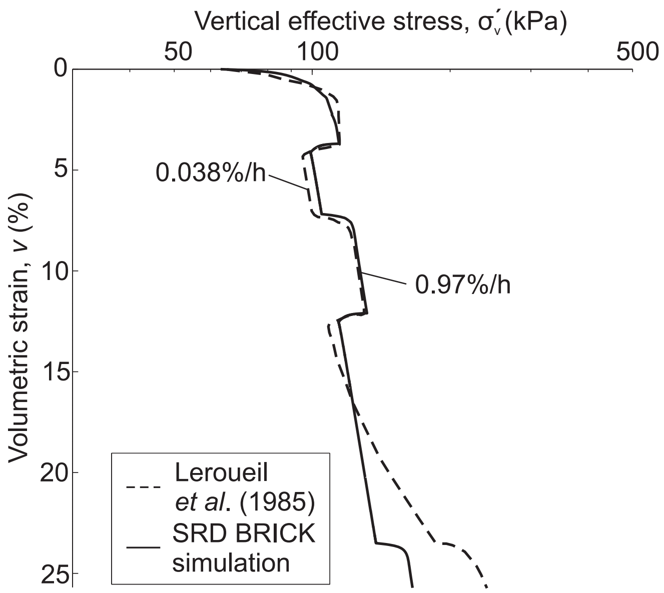

Vertical effective stress, σ'_v (kPa)
50
100
500
0
5
10
15
20
25
Volumetric strain, v (%)
0.038%/h
0.97%/h
Leroueil
et al. (1985)
SRD BRICK
simulation

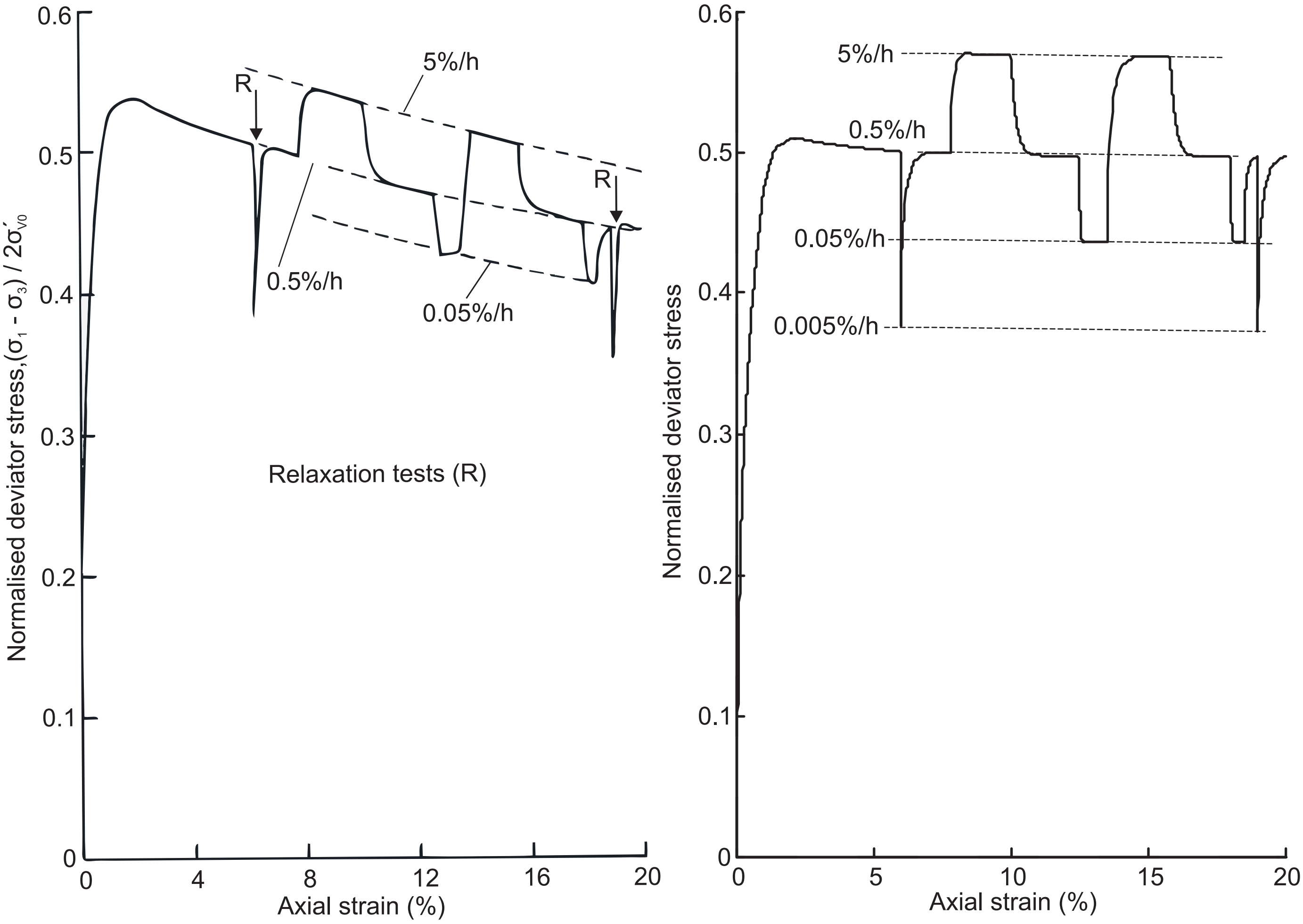

0.6
0.5
0.4
0.3
0.2
0.1
0
Normalised deviator stress,(σ1 - σ3) / 2σ′V0
R
5%/h
0.5%/h
0.05%/h
R
Relaxation tests (R)
0
4
8
12
16
20
Axial strain (%)
0.6
0.5
0.4
0.3
0.2
0.1
0
Normalised deviator stress
5%/h
0.5%/h
0.05%/h
0.005%/h
0
5
10
15
20
Axial strain (%)

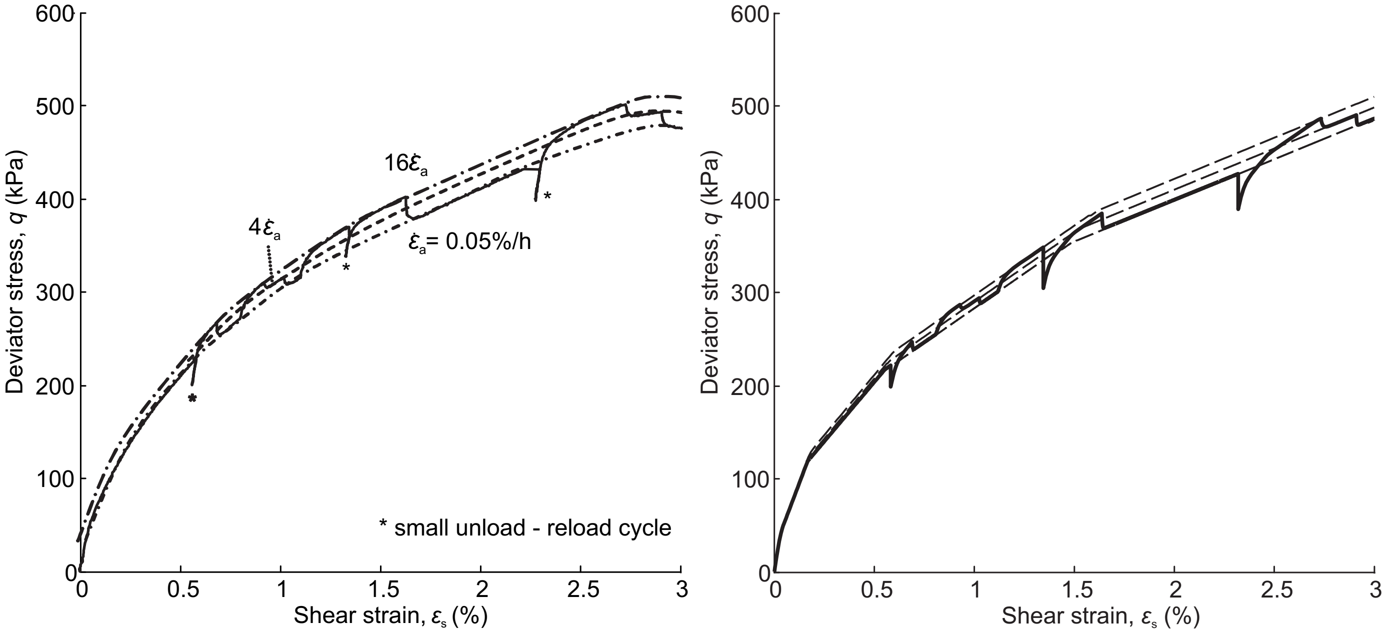
Deviator stress, q (kPa)
Shear strain, εs (%)
16ε̇a
4ε̇a
ε̇a= 0.05%/h
* small unload - reload cycle
0
100
200
300
400
500
600
0.5
1
1.5
2
2.5
3

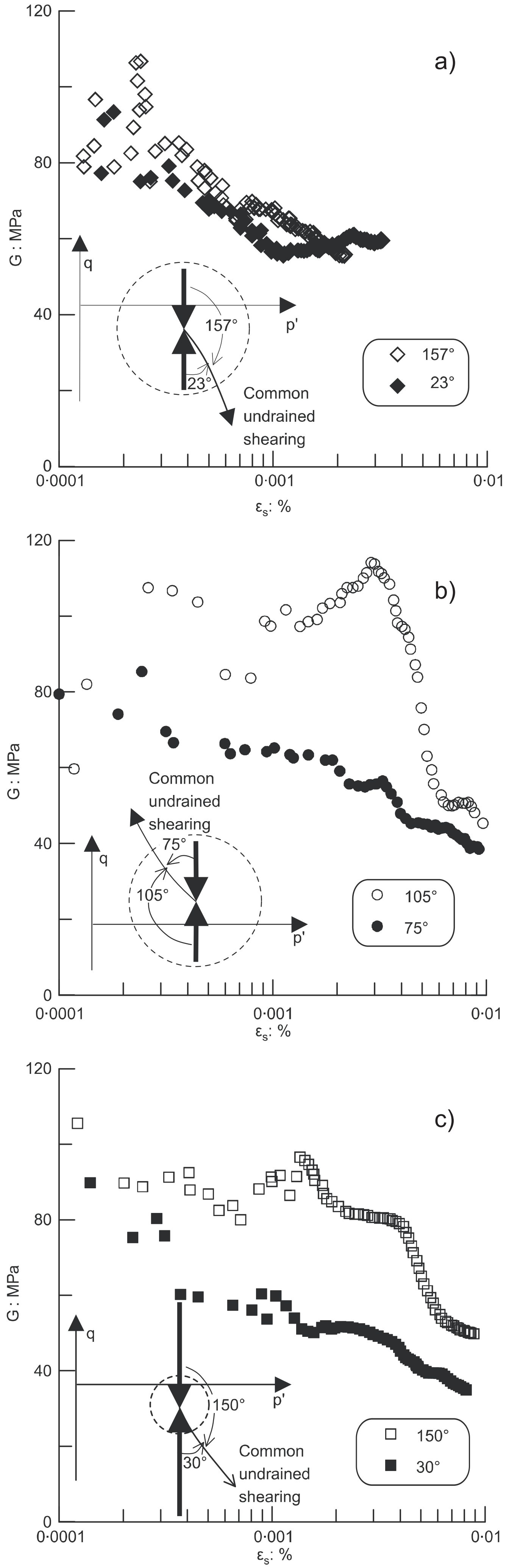

a)
G : MPa
120
80
40
0
0·0001
0·001
0·01
εs: %
q
p'
157°
23°
Common
undrained
shearing
157°
23°
b)
G : MPa
Common
undrained
shearing
75°
105°
105°
75°
c)
150°
30°
Common
undrained
shearing
150°
30°

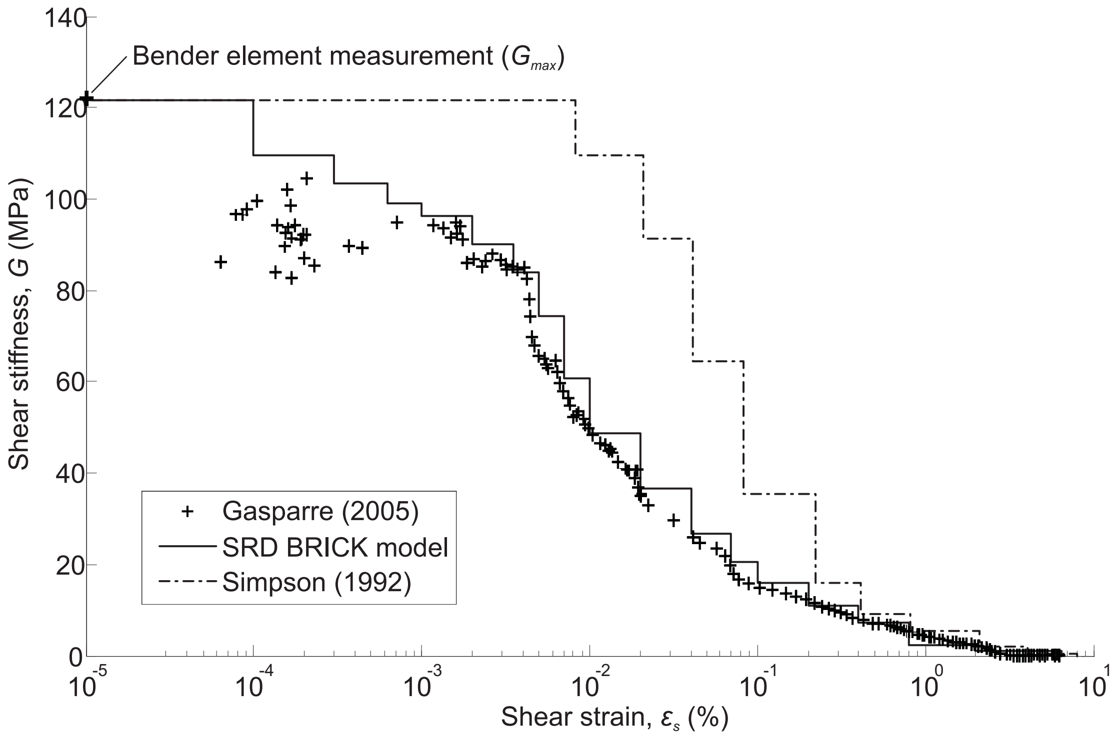

Bender element measurement (G_{max})
Shear stiffness, G (MPa)
Shear strain, ε_s (%)
Gasparre (2005)
SRD BRICK model
Simpson (1992)
140
120
100
80
60
40
20
0
10^{-5}
10^{-4}
10^{-3}
10^{-2}
10^{-1}
10^{0}
10^{1}

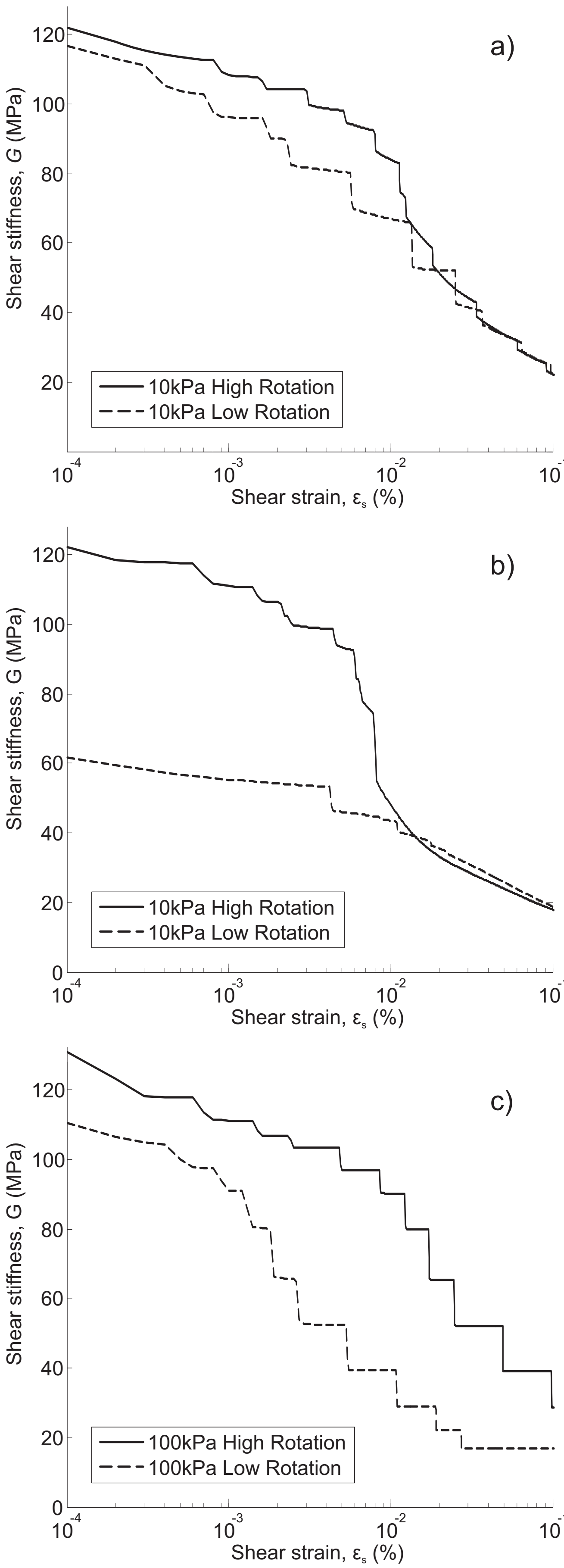

a)
Shear stiffness, G (MPa)
120
100
80
60
40
20
10kPa High Rotation
10kPa Low Rotation
10^{-4}
10^{-3}
10^{-2}
10^{-1}
Shear strain, ε_s (%)
b)
Shear stiffness, G (MPa)
120
100
80
60
40
20
0
10kPa High Rotation
10kPa Low Rotation
10^{-4}
10^{-3}
10^{-2}
10^{-1}
Shear strain, ε_s (%)
c)
Shear stiffness, G (MPa)
120
100
80
60
40
20
0
100kPa High Rotation
100kPa Low Rotation
10^{-4}
10^{-3}
10^{-2}
10^{-1}
Shear strain, ε_s (%)